Assessing urban thermal field variance and surface urban heat island effects. An Ecological Study in Malakand Division, Pakistan

Évaluation de la variance du champ thermique urbain et des effets d'îlot de chaleur urbain de surface. Une étude écologique dans la Division de Malakand, au Pakistan

Imtiaz AHMAD[1,2], Wang PING[1,2*], Abdur RAZZAQ[3], Bilal Jan Haji MUHAMMAD[1,2], Wajid ALI[3]

[1] Key Laboratory of Geographical Processes and Ecological Security in Changbai Mountains, Ministry of Education, School of Geographical Sciences, Northeast Normal University, Changchun, China.
[2] School of Geographical Sciences, Northeast Normal University, Changchun 130024, China.
[3] School of Environment, Northeast Normal University, Changchun, China.

* Correspondence to: wangp666@nenu.edu.cn.

CC BY 4.0

Vol. 34.2 / 2024, 61-88

GEOREVIEW

Received:
8 October 2024

Accepted:
13 December 2024

Published online:
17 December 2024

ABSTRACT: This study examines the ecological and thermal impacts of urbanization in Malakand Division, Pakistan, from 2003 to 2023, focusing on the Surface Urban Heat Island (SUHI) effect and human thermal comfort (HTC). Using multi-temporal Landsat (5 & 8) imagery, Land Surface Temperature (LST) data, and the Urban Thermal Field Variance Index (UTFVI), we analyze urban expansion, land-use changes, and their thermal implications. Results show significant urban growth, with built-up areas increasing from 11,773.5 km² to 12,519.09 km², while vegetative land decreased by 7.5%. The average LST rose by 3.67°C, and UHI intensity increased from 15.96% in 2003 to 19.08% in 2023. Spatial analysis highlights higher LST and UTFVI values in urbanized and transition zones, indicating worsening thermal conditions. These findings underscore the need for sustainable urban planning to mitigate UHI effects, enhance HTC, and promote green space development. This research provides critical insights for urban planners and policymakers in Malakand Division and other rapidly urbanizing regions.

KEY WORDS: Ecological Monitoring, LST, UHI, UTFVI, Human thermal comfort.

RÉSUMÉ : Cette étude examine les impacts écologiques et thermiques de l'urbanisation dans la division de Malakand, au Pakistan, de 2003 à 2023, en se concentrant sur l'effet des îlots de chaleur urbains (ICU) et le confort thermique humain (CTH). En utilisant des images satellites Landsat (5 & 8), des données de température de surface (LST) et l'Indice de Variance du Champ Thermique Urbain (UTFVI), nous analysons l'expansion urbaine, les changements d'usage des sols et leurs implications thermiques. Les résultats montrent une croissance urbaine significative, avec une augmentation des zones bâties de 11 773,5 km² à 12 519,09 km², tandis que les terres végétatives ont diminué de 7,5 %. La température moyenne de surface a augmenté de 3,67°C et l'intensité de l'ICU a augmenté, passant de 15,96 % en 2003 à 19,08 % en 2023. L'analyse spatiale met en évidence des valeurs plus élevées de LST et d'UTFVI dans les zones urbanisées et de transition, indiquant une dégradation des conditions thermiques. Ces résultats soulignent la nécessité d'une planification urbaine durable pour atténuer les effets de l'ICU, améliorer le CTH et promouvoir le développement des espaces verts. Cette recherche fournit des informations essentielles pour les urbanistes et les décideurs politiques de la division de Malakand et d'autres régions en forte urbanisation.

MOTS CLÉS: Surveillance écologique, LST, UHI, UTFVI, Confort thermique humain.

How to cite this article:
Ahmad, I., Ping, W., Razzaq, A., Muhammad, B.J.H., Ali, W. (2024) Assessing urban thermal field variance and surface urban heat island effects. An Ecological Study in Malakand Division, Pakistan. Georeview, 34, 2, https://doi.org/10.4316/GEOREVIEW.2024.02.05

1. Introduction

Metropolitan regions are increasingly becoming central hubs for human habitation and diverse economic and social activities. These urban centers have a profound influence on the economic, cultural, and political landscape of the world. According to a study by Liang et al2021), the growing importance of cities is inescapable as they serve as focal points for human residence, driving economic activities and shaping societal developments. Currently, over 56% of the global population resides in metropolitan areas, and this number is projected to increase significantly by 2050, with urban populations expected to rise to 5 billion individuals. This will account for approximately 70% of the world's total population (United Nations, 2018). This ongoing urbanization trend presents both opportunities and challenges that are key to understanding the future of human settlements and the world's ecological balance.

The rapid urbanization process involves substantial changes in land use patterns, resulting in the conversion of natural surfaces, such as vegetation, water bodies, and permeable soils, into impervious surfaces such as buildings, roads, and other forms of infrastructure (Kafy, Rahman, et al., 2021; Qu et al., 2020). These modifications not only alter the physical landscape but also have a profound impact on the environmental frameworks of cities, including the microenvironments that exist within them (Imran et al., 2022). The shift from natural landscapes to urbanized areas impacts local and regional ecosystems, altering ecological balances and disrupting energy fluxes on the Earth's surface, ultimately affecting the global climate system (Jain et al., 2017).

Urbanization, as discussed by Abir et al. (2021), has a dual nature, offering both economic and social benefits but also posing significant environmental and ecological challenges. The economic advantages of urbanization are undeniable, providing opportunities for job creation, industrial growth, and the advancement of infrastructure. However, the environmental costs are equally substantial, as urbanization often leads to the destruction of habitats, loss of biodiversity, and degradation of natural resources (Gazi et al., 2021; López et al., 2001). These consequences manifest in various forms, such as the reduction in green spaces, the deterioration of ecological conditions, and the rise of urban heat islands (UHI). Further environmental issues include the pollution of air and water, the reduction of agricultural lands, and the transformation of previously natural landscapes into impermeable surfaces that exacerbate stormwater runoff and heat retention (Nguyen et al., 2019).

The changes brought about by urbanization also significantly affect the climatic conditions within cities. As natural landscapes are replaced with built environments, the microclimates of cities experience shifts, leading to increased energy consumption, a decrease in rainfall, and rising surface temperatures and humidity levels (Abir et al., 2021). Urban areas are known to absorb more solar radiation than their rural counterparts, leading to a phenomenon known as the Urban Heat Island (UHI) effect, where the temperature in urban areas is significantly higher than that of surrounding rural areas (Martin et al., 2015). These areas, due to their built environment, have an increased capacity to absorb and retain heat, making them more susceptible to temperature extremes.

The process of urbanization exacerbates the phenomenon of Urban Heat Islands (UHIs), largely because of the inherent properties of impervious surfaces—such as roads and buildings—that are commonly found in cities. These surfaces are characterized by low reflectivity and high heat-retaining properties, which contribute to the accumulation of heat in the urban environment (Sahana et al., 2016; Ullah et al., 2019). These surfaces absorb heat during the day and release it slowly at night, causing urban areas to experience higher surface and air temperatures compared to surrounding natural or rural regions (Alfraihat et al., 2016). This alteration of land surface

temperature (LST) is a critical factor in the development of UHI, and as cities expand, their capacity to absorb and retain heat increases, amplifying the intensity of these temperature disparities.

The UHI effect is not only a function of urban infrastructure but also results from the thermal energy generated by human activities. Liu et al. (2020) explain that the combination of urban characteristics—such as the presence of concrete and asphalt—and anthropogenic activities, such as transportation, industrial processes, and the use of energy-consuming appliances, generates additional thermal energy that further elevates temperatures in cities. Over time, the buildup of heat in urban areas exacerbates the UHI effect, contributing to higher overall temperatures and creating an environment that is uncomfortable for residents.

The existence of UHI effects can have far-reaching consequences. As detailed by Gherraz et al. (2020) and Rooney et al. (1998), these temperature increases are not limited to human discomfort but also have a significant impact on local weather patterns and ecosystems. The urban heat island effect is associated with increased energy consumption, as residents and businesses seek to cool their environments through air conditioning and other forms of cooling systems. This increased energy demand, in turn, can lead to higher emissions of greenhouse gases, further contributing to global warming (Alfraihat et al., 2016). Additionally, the elevated temperatures contribute to heatwaves, which have meteorological consequences such as increased frequency and intensity of storms, as well as shifts in precipitation patterns (Gherraz et al., 2020; Rooney et al., 1998).

Surface intensity islands, which are a key characteristic of the UHI effect, form as a result of a combination of factors, including high population density, human activities, local meteorological conditions, and geographical features (Mohajerani et al., 2017; Wemegah et al., 2020). The UHI effect is typically assessed at multiple levels, including the canopy layer, outer urban areas, and surface levels (Oke, 1976; Zhang et al., 2009). To accurately measure and assess UHI, researchers have used a variety of techniques, including remote sensing and satellite imagery, which allow for the calculation of temperature differences between urban and non-urban areas (Mirzaei & Haghighat, 2010; Voogt, 2007). These studies aim to quantify the extent of the UHI effect at the mesoscale, providing valuable insights into the factors that contribute to urban warming and its environmental impacts.

The UHI effect is known to exacerbate several environmental issues, such as the degradation of water quality, increased pollution levels, and elevated concentrations of greenhouse gases (Voogt & Oke, 2003). These changes not only affect human health and well-being but also disrupt local ecosystems, causing harm to vegetation, wildlife, and the broader ecological balance of urban areas. In regions such as Malakand Division, urbanization patterns are similar to those observed globally, where rapid urban growth is replacing natural landscapes with impermeable surfaces, leading to significant consequences for the environment and microclimates. These transformations underscore the need for sustainable urban planning strategies that can mitigate the adverse effects of UHI and promote healthier urban environments (Venter et al., 2020).

To assess the UHI effect, various metrics have been developed, such as the Metropolitan Warm Field Difference List (UTFVI), a mathematical model that uses surface temperature data to measure the extent of UHI in metropolitan areas (Sobrino & Irakulis, 2020). According to Nguyen et al. (2019) and Portela et al. (2020), UTFVI is widely recognized as an effective tool for assessing environmental conditions in urban areas, as it allows for a more accurate understanding of urban thermal comfort and ecological health. The UHI phenomenon is associated with a wide range of negative consequences, including declining air quality, variations in humidity, reduced thermal comfort, increased mortality rates, and shifts in local atmospheric circulation (Buchori; Kafy, Rahman, et al., 2021; Singh et al., 2017). The use of metrics like UTFVI is essential in creating strategies for sustainable urban development and mitigating the harmful effects of UHI.

In the context of Malakand Division, urbanization has led to significant increases in air and surface temperatures. Since the early 1980s, the rapid growth of urban areas, along with the expansion of industry, commercial enterprises, and residential developments, has resulted in elevated temperatures. These changes have been further exacerbated by the destruction of vegetation, deforestation, and the increased use of electrical devices and vehicles (Mumtaz et al., 2020; Qureshi et al., 2012; Shah & Ghauri, 2015). The resultant rise in surface and air temperatures has impacted the comfort of residents and posed challenges to urban planning and environmental sustainability.

Despite the growing recognition of UHI and its consequences, there remains a gap in research examining the effects of UHI in Malakand Division, particularly in terms of the Urban Thermal Field Variation Index (UTFVI) and the Ecological Evaluation Index (EEI). This study aims to address this gap by exploring the impacts of land use changes, land surface temperature (LST), urban heat islands (SUHI), and urban vegetation coverage (UTFVI) on the ecological and climatic conditions of the region (Maithani et al., 2020). By analyzing satellite imagery from 2003 to 2023, the study will offer valuable insights into the urban heat environment of Malakand Division, thereby informing future urban planning and sustainable development strategies that prioritize human health, environmental quality, and ecological sustainability.

The findings from this study will be crucial for advancing improved urban design and planning techniques that take into account the adverse effects of urban heat islands. Addressing these challenges will not only enhance the quality of life for residents but also contribute to the broader goals of sustainable urban development and climate resilience (Shakrullah, 2020).

The examination aims to accomplish the following objectives: The objectives of this investigation are as follows: (1) The objective is to analyze the changes in (LST) over time and space using thermal band data from Landsat. (2) The aim is to examine how the (UHI) effect affects different surface cover scenarios and regions. (3) The goal is to evaluate the environmental and thermal conditions of Malakand Division using the (UTFVI). (4) The purpose is to investigate the relationship between land-use indices and LST. (5) The objective is to quantitatively assess the environmental impact of UHI using both the UTFVI and the (EEI). The purpose of this study is to conduct a thorough analysis of the long-term patterns of (UHI) and the correlation between the urban thermal environment (UTE) and many factors that impact it. Furthermore, it intends to investigate the favorable ecological conditions in the Malakand Division.

2. Study Area

This study is centered on the Malakand Division (Fig. 1) in the Khyber Pakhtunkhwa province of Pakistan. The division includes districts such as Swat, Dir, and Chitral. The region exhibits diverse topography, ranging from flat plains to rugged mountainous terrain, including an area of approximately 9,528 square kilometers. The division exhibits varying population densities, with the valleys being more heavily populate The elevations in the Malakand Division vary from approximately 600 meters to around 3,500 meters above sea level and the mountainous parts having few inhabitants. The climate displays significant fluctuations, with winter temperatures dropping to 5°C and temperatures during the summer soaring to 30°C.In the peak months of May and June, maximum temperatures can soar up to 58°C. December and January are the months with the lowest temperatures, sometimes reaching as low as 0°C.

Urbanization in the last twenty years has caused notable alterations in land utilization, as urban plant life has been substituted by non-porous buildings and residential zones, leading to an 18% rise in developed areas. The urban vegetation in Malakand Division is diverse and includes a variety of

green spaces, such as playgrounds, Parkland, green spaces, public gardens, cultivated land, and areas with both sparse and dense grasslands. Progression in the area has experienced significant growth and widespread construction.

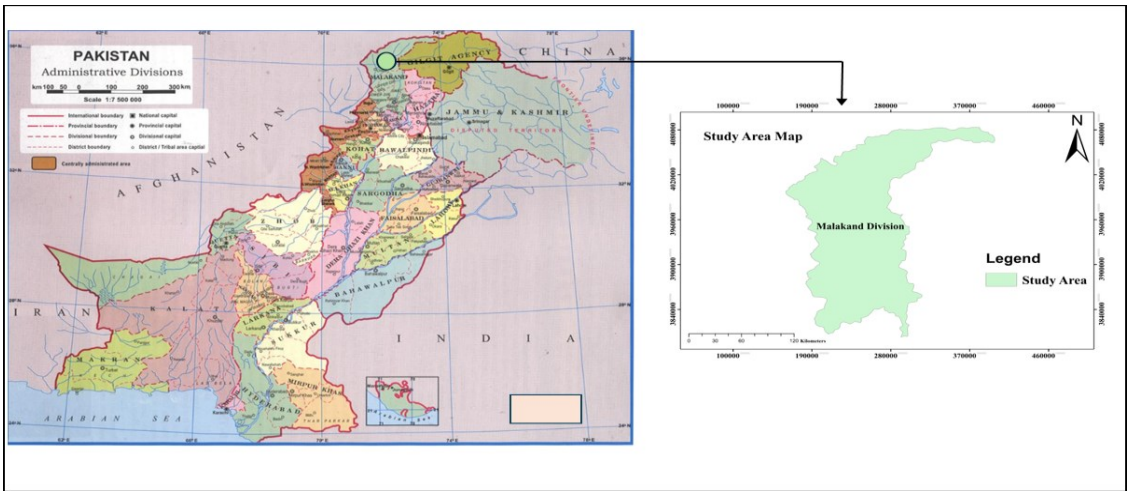

Figure 1 The study area's (Malakand Division) geographic location.

3. Methods

Preprocessing of Data source

This study utilized Landsat satellite data from multiple time periods, specifically from the Landsat 5 (TM), Landsat 8 (OLI), and Warm Infrared Sensor (TIRS), to examine changes in (LULC), temperature fluctuations, (UHI) effects, and (UTFVI). The examination utilizes three Landsat photographs: two photos captured by the Landsat 5 (TM) sensor in 2003 and 2013, and imagery obtained by the Landsat 8 (OLI-TIRS) sensor in 2023 (Fig. 2). The picture selected for the Spring period was carefully chosen to accurately represent the characteristics of the spring season. This was achieved by mitigating the impact of cooling and warming and maximizing the extent of the tree's shade. This excerpt allows for the differentiation between areas with abundant plant life and those that are abandoned and unproductive (Abir et al., 2021; Shah & Ghauri, 2015). The use of band 10 of Landsat 8 to determine land surface temperature is not completely reliable, as advised to the USGS.

In addition, the review area of Malakand Division was employed for the analysis of all Landsat images, as well as various datasets such as Land Use (LU), (NDVI), Standardized Contrast Built Index (NDBI), Standardized Contrast Water Index (NDWI (LST), (UHI), and (UTFVI), which were generated for further examination at the divisional level. Each satellite symbol was subjected to corrections for potential presence of distorted pixels caused by aerial, mathematical, and radiological factors. Table 1 presents a summary of the three Landsat datasets that were used in this investigation.

The "Strategies" section outlines the guidelines for organizing land use (LU), eliminating (LST), evaluating the extent of UHI evaluating urban heat and vegetation data in the form of a metropolitan heat field difference file, and investigating the relationship between (LU) lists and LST. The objective of the review is to evaluate the Metropolitan Intensity Island (UHI) and Metropolitan Tree Fracture and Vegetation File (UTFVI) using the purposeful (LST) collected from thermal clusters. The land utilizes surface records, such as (NDVI) (Normalized Difference Vegetation Index), (NDBI) (Normalized Difference Built-up Index), and (NDWI) (Normalized Difference Water Index), are employed to analyze the variations in different land categories, such as built-up areas, barren lands,

vegetated lands, wetlands, sparse vegetation, and water bodies. These records are also utilized to assess their correlation with (LST). The technique of SLRM is employed to evaluate the influence of each indicator on several aspects of the study area. The UPGMA approach is employed to evaluate and delineate the (EEI) for Malakand Division. The system is illustrated in a flowchart (Fig. 3) and explained in the following section.

Table 1 Data acquisition details of Landsat images.

Year	Acquired date	Satellite sensor	Band	Spatial resolution		Cloud cover
				Multi-spectral	Thermal bands	
2003	18-March-2003	Landsat (5) Thematic Mapper (TM)	1–5 and 7	30 m	30 m (resampled from 120)	0%
			6	-		
			Pan 8	15 m	-	
2013	07-March-2013	Landsat (5) Thematic Mapper (TM)	1–5 and 7	30 m	-	0%
			6	-	30 m (resampled from 120)	
			Pan 8	15 m	-	
2023	15-March-2023	Landsat (8) Operational Land Imager (OLI)	1–8	30 m	-	5.22%
			Pan 9	15 m	-	

Source: http://earthexplorer.usgs.gov/

The picture was partitioned into distinct land-use (LU) categories using various classification methods. Common techniques for aggregating data from sensors include the supervised maximum likelihood classifier (MLC), random forests (RF), K-means clustering, deep learning algorithms, fuzzy logic, and artificial neural networks (ANN) (Talukdar et al., 2020). The survey employed a probabilistic technique and a systematic pixel-based calculation to conduct an analysis of land use and land cover (LULC). The survey district is divided into six primary land-use categories: urbanized areas (consisting of buildings, roads, and other non-permeable surfaces), vegetation (including urban green spaces, agricultural land, forests, shrubs, and other plant-covered surfaces), barren land (comprising of sand, bare soil, and areas without natural vegetation), and water resources (including lakes, ponds, rivers, streams, and other wetlands).

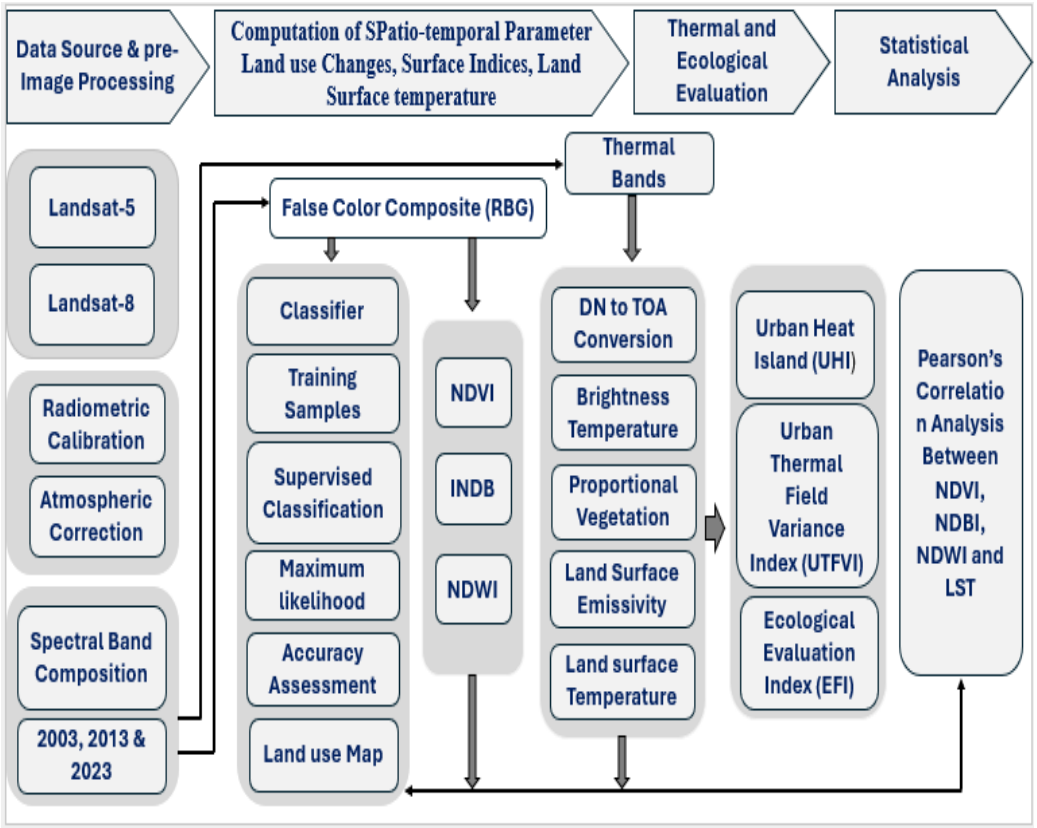

Figure 2 Methodology flow chart of the study.

4. Assessment of Accuracy

The precision of the land use and land cover (LULC) plan map was assessed using various metrics, such as overall accuracy, user accuracy, producer's accuracy, and the Kappa coefficient (Zia, 2014). To evaluate the accuracy of each planned land use map, a total of 250 random samples were selected using Google Earth imagery. The Kappa calculations were utilized to assess the accuracy of the LU maps, as presented in Table 2. The reliability for each testing period consistently over 90%, and the Kappa coefficient values for all three years exceeded 0.85. A Kappa coefficient of 0.75 indicates a high level of precision, as stated by Pontius and Millines (2011). Table 1 displays the various complexities of the Landsat clusters that are utilized to validate surface temperature observations in the Malakand Division. The computerized numbers (DN) for Landsat 5(TM) and 8(TIRs) were initially calibrated using the approach outlined in conditions (1) and (2) provided in the sensor handbooks (USGS, 2019). The LST was resolved utilizing the accompanying methodology:

Transformation of DNs to Otherworldly Brilliance (Lλ)

Landsat 5.TM, Eq. (1) changes over the DNs into ghostly brilliance (Lλ) values (USGS, 2019):

$$L_\lambda = L_{MIN} + (L_{MAX} - L_{MIN}) \times \text{DN}/255 \quad (1)$$

Here, Lλ represents the spectral radiance at the sensor's aperture. LMAX (15.6 for 5-TM) and LMIN (1.238 for 5-TM) denote the maximum and minimum spectral radiance values, respectively, scaled to QCALMAX and QCALMIN.

For Landsat 8-TIRs, DNs are converted to spectral radiance (Lλ) values using Eq. (2) (USGS, 2019):

$$L_\lambda = M_L * Q_{CAL} + A_L \quad (2)$$

Let Lλ represent the extraordinary brightness at the sensor's opening for a specific band. ML is the factor used to multiply the brightness (0.0003342), while AL is the factor used to add to the brightness (0.1). QCAL refers to the standard pixel values in DN for band 10, which were quantized and aligned.

Transcendent luminosity transforming into resplendent temperature variation.

The obtained extraordinary luminosity (Lλ) values are used to evaluate the brightness temperature at the satellite in Kelvin. To convert these properties entirely to Celsius (°C), Equation (3) is subtracted by 273.15 (Joshi & Bhatt, 2012).

Table 2 LULC accuracy assessment.

Year	User Accuracy	Producer Accuracy	Overall Accuracy	Kappa Coeifficient
2003	91.74	92.03	92.59	91.49
2013	92.25	93.21	94.27	92.75
2023	91.56	92.13	92.86	90.64

Estimation of LST

The temperature brightness (TB) at the satellite is calculated in Celsius using the following equation:

$$T_B = K_2 n\,(K_1/L_\lambda + 1) - 273.15 \quad (3)$$

LST is then derived from TB using:

$$\text{LSE } (\varepsilon) = 0.004 * P_V + 0.986 \quad (4)$$

where TB is the brightness temperature in Celsius, and K1 and K2 are calibration constants specific to the sensors used: 607.76 and 1260.56 for Landsat 5-TM, and 774.89 and 1321.08 for Landsat 8-TIRs, respectively (Sameen & Al Kubaisy, 2014). Lλ represents the spectral radiance at the sensor's aperture. λ, the wavelength of emitted radiance, is 11.45 µm, and ρ is 14,380.

Estimation of Land Surface Emissivity

The land surface emissivity (ε) should be adapted to elements like design, harshness, and surface (Giannini et al., 2015; Sobrino et al., 2004). The NDVI-based emissivity remedy is applied utilizing:

ε=0.004·PV+0.986ε = 0.004 \cdot PV + 0.986ε=0.004*PV +0.986

where PV is the extent of vegetation, determined as:

$$P_v = [(NDVI - NDVI_{min}) / (NDVI_{max} - NDVI_{min})]^2 \quad (5)$$

Pixels are ordered considering NDVI values: values more prominent than 0.5 are completely vegetated (doled out 0.99), while values somewhere in the range of 0.2 and 0.5 are somewhat vegetated.

Estimation of Land Surface Records

To explore the relationship between LULC changes and LST, indices such as NDVI, NDBI, and NDWI are used. The NDBI, which measures built-up area density, is calculated as:

NDVI, a key indicator for vegetation density, is calculated using:

$$NDVI=NIR - Red/NIR + Red \quad (6)$$

NDWI is used to extract water bodies, calculated as:

$$NDWI = (Green - NIR) / (Green+NIR) \quad (7)$$

Using PV from the NDVI calculation and the emissivity estimate from the previous equation, the emissivity (ε) is determined through linear regression.

Estimation of UHI and UTFVI

The (UHI) and (UTFVI) are assessed utilizing the adjusted upsides of land surface emissivity (ε). Because of between yearly vacillations and shifting air conditions, symbolism from various years is standardized utilizing:

$$UHI = Ts - Tm/SD \quad (8)$$

This standardization guarantees that pictures from various years are equivalent (Zhang et al., 2001).

UHI and UTFVI Estimation

The (UHI) impact is evaluated utilizing the condition:

$$UTFVI = Ts — Tm/Tm \quad (9)$$

Let Ts represent the land's surface temperature, Tm denote the average surface temperatures of the region, and SD represent the standard deviation. A place is considered to have a Metropolitan Intensity Island if its normalized parameters exceed the average Lands Surface Temperature by more than 1 °C. To gain a clearer understanding of the Urban Heat Island (UHI) phenomenon in a specific survey area, several studies (Zhang et al., 2009). Utilize the following formula to quantitatively analyze the Urban Thermal Footprint Vegetation Index (UTFVI) (Naim & Kafy, 2021).

The formula UTFVI calculates the difference between Ts and Tm, divided by Tm.UTFVI is the abbreviation for "Uniform Time Frame Volume Indicator". The equation (10) can be rewritten as UTFVI = Tm(Ts - Tm). In this unique situation, Ts represents the least squares estimate (LST) value, and Tm is the average LST of the survey area (Singh et al., 2017). The desired UTFVI values are determined based on the EEI, which ranges from excellent to extremely poor (Renard et al., 2019; Sharma et al., 2021).

Data Limitations

The research encountered specific obstacles, such as the limited resolution of satellite images, the lack of meteorological data from only two weather monitoring stations within the study area, and inadequate land-use data, which impeded a comprehensive and meticulous analysis. Furthermore, the audit failed to adequately depict the influence of urban essential factors, including differences in building density, height, and land use. In subsequent evaluations, it will be necessary to align these parameters due to their significant influence on heat island effects.

Findings on the dynamics of urban land use change

Urbanization is the primary driving force behind alterations in the Earth's surface, continuously modifying and reconfiguring how land is used and covered due to Human endeavors (Corner et al., 2014; Meshesha et al., 2016), and resulting in severe weather conditions (Nath et al., 2020). This study investigates the instances of urban land use modifications and their implications for the hot climate. Figure 4 illustrates the distribution of land utilization in the exploration zone Utilizing Landsat imagery for the specified period 2003, 2013, and 2023. The exploration locality has a total area of 9,528 square kilometers, with vegetation being a prominent land-use category. The vegetation cover has decreased from 14.8497% in 2003 to 13.861% in 2023. However, the amount of man-made land in the Malakand Division has nearly doubled in the past twenty years. The land area has increased from 11,773.5 km² in 2003 to 12,519.09 km² in 2023, representing a rise in land extent from 43.10451% to 45.837% (Table 3). The increase in size is mostly attributed to the proliferation of impermeable surfaces, particularly in the northeast, southeast, and southwest parts of the territory (Fig. 4). The primary driving force behind land-use modification in the Malakand Division is the significant increase of impermeable surfaces.

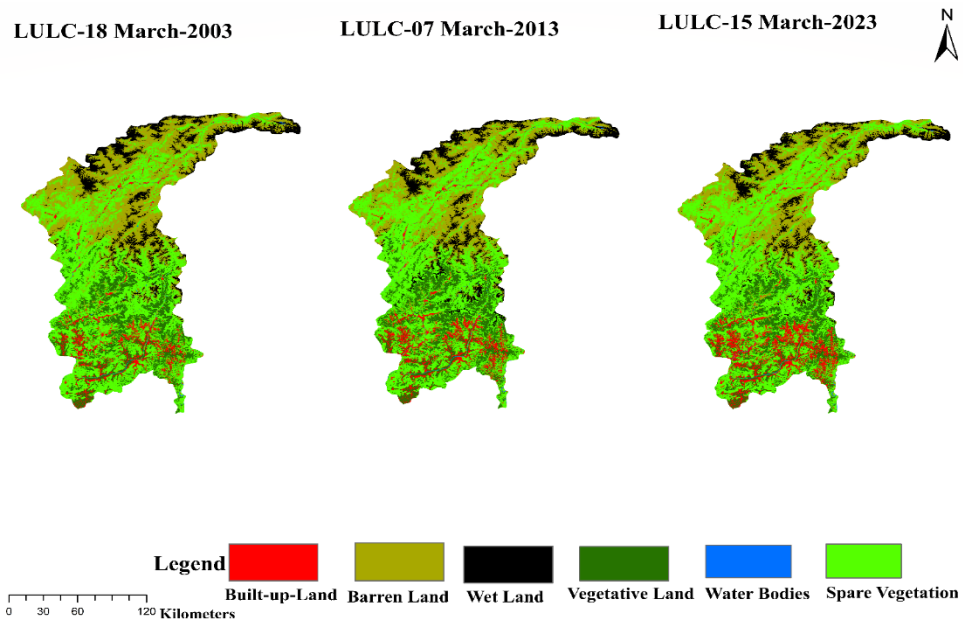

Figure 3 Land-use map of Malakand Division in 2003, 2013, and 2023.

Table 3 Analysis of Land-Use Dynamics from 2003 to 2023.

	2003		2013		2023		2003-2023
	Area (km²)	% Age	Area (km²)	% Age	Area (km²)	% Age	% Change
Water Bodies	123.599	0.4525	117.302	0.42946	110.136	0.4032	-0.04928
Vegetative Land	4091.19	14.9784	3835.19	14.041	3786.24	13.861	-0.1791
Spare vegetation	1300.68	4.76198	1601.39	5.8629	2005.05	7.3424	-2.58042
Barren Land	7568.6	27.7097	6465.54	23.6712	6347.05	23.2374	-4.475
Wet Land	2774.69	10.15855	2881.03	44.51	2482.64	9.08929	1.06926
Built-up-Land	11773.5	43.10451	12154.4	445100	12519.09	45.837	-2.73249

Between 2003 and 2023, there was a significant increase in developed land and surfaces that cannot be penetrated, while the amount of exposed land declined from 27.7097% to 23.2374%, and the area covered by water bodies decreased from 0.4525% to 0.4032%. The decrease in vacant land is due to the development of housing and commercial projects as well as urban expansion in the Malakand Division. A substantial portion of the barren and arable terrain has been converted into developed areas.

Figure 4 indicates that Extra Desolate Land and rural terrains in the southern and southwestern parts of the territory have been transformed into impassable surfaces. By 2023, the developed region is projected to have increased its vegetative cover and expanded its use of infertile land, as indicated in Figure 4. These patterns illustrate the extensive impact of urbanization throughout Malakand Division.

Analysis of Dynamics in LST Change

The LST in Malakand Division was evaluated utilizing Landsat thermal band data for the years 2003, 2013, and 2023. The LST maps indicate that temperature variations in the research area have grown due to variables such as urbanization and extreme weather conditions (Amiri et al., 2009; Sekertekin et al., 2016). The analysis revealed that the Land Surface Temperature (LST) for all categories experienced a rise from 2003 to 2023. This increase was primarily caused by an uneven distribution of impermeable surfaces and urban vegetation cover, as seen in Table 4. Additionally, the effects of climate change and global warming further intensified this situation. The broad extension of metropolitan regions has changed an enormous part of horticultural land and metropolitan green spaces into created or useless land, subsequently compounding the expansion in Land Surface Temperature (LST).

During period from 2003 to 2023, notable fluctuations in LST were detected. In 2013, the lowest recorded LST was -33.57°C. By 2023, it had increased to -32.94°C, showing a rise of roughly -35.18°C during this time. The minimum land surface temperature (LST) in 2003 was recorded at -35.18°C. By 2023, it had reduced to -32.94°C, indicating a reduction of -2.24°C. On the other hand, the highest Land Surface Temperature (LST) rose from 57.37°C in 2003 to 58.36°C in 2023. Through the examination of the fluctuations in average LST over a period of time, a more distinct and discernible pattern becomes evident. The LST values for these decades 2003, 2013, and 2023 were 18.26°C, 18.91°C, and 19.42 °C, respectively, as indicated in Table 4. Table 4 demonstrates a consistent rise

in average Land Surface Temperature (LST) of 1.16°C over a span of 20 years, which equates to a 2% increase since 2003.

The changing trends are illustrated by the LST maps of Malakand Division shown in Figure 5. The maps employ a color gradient ranging from deep brown to pale yellow to depict progressively higher to lower Land Surface Temperature (LST) readings. The degree of the dull earthy colored area in the 2013 LST map (Fig. 5) is more noteworthy than that in the 2003 picture (Fig. 5), recommending an expansion in the size of regions with raised land surface temperature (LST). The trend persisted, showing a substantial rise in locations with high Land Surface Temperature (LST) in 2023 (Fig. 5). This scenario exemplifies the disparity in Land Surface Temperature (LST) over the Malakand Division. By 2023, there was a noticeable escalation in the intensity of metropolitan Heat Island (UHI), resulting in higher temperatures within the central metropolitan regions. The expansion in temperatures can be credited to the extension of the metropolitan developed area.

Table 4 Analysis of Land Surface Temperature (LST) Metrics and Change Rat.

Year	Minimum	Maximum	Mean	SD	Change rate
2003	-35.18	57.37	18.26	15.8	34.31%
2013	-33.57	57.98	18.91	15.9	32.26%
2023	-32.94	58.36	19.42	18.1	33.41%

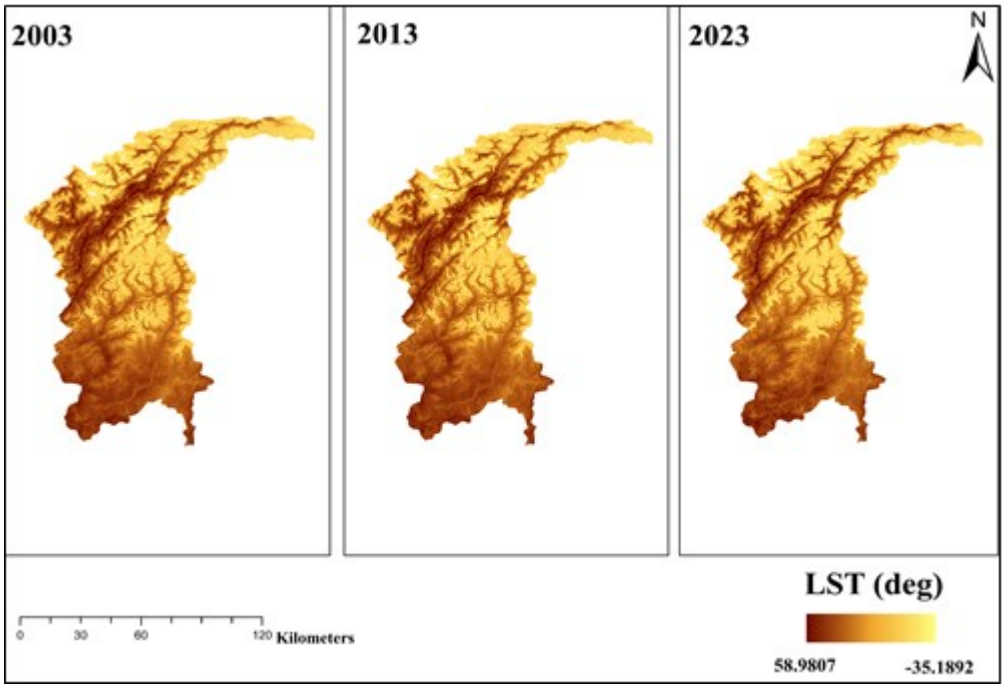

Figure 4 Spatiotemporal patterns of LST in **2003**, **2013**, and **2023.**

The creation of urban areas has impacted the (UHI) effect and made natural hazards more apparent in the research area, as measured by the (UTFVI). Vegetation and the execution of urban greening

efforts improve thermal comfort. Nevertheless, the study area has experienced elevated (UHI) values due to the confluence of a dense population and alterations in urban land utilization.

LST Distribution in Different LU Classes

Figure 6 depicts the spatial and temporal distribution of LST) in different land use (LU) categories in the Malakand Division from 2003 to 2023. The study found that the average (LST) increased because there was an unequal distribution between built-up area and urban vegetation. In 2023, the land that is resistant to penetration displayed the highest LST), while bodies of water had the lowest LST across the different land use (LU) classes. The mean surface temperature (LST) of aquatic bodies increased from 3.79°C in 2003 to around 3.85°C by 2023. The Vegetation (LST) had a significant increase from 12.52°C in the year 2000 to a value of 16.61°C by the year 2023.

In 2023, the "Transition Zone," a newly identified land-use classification consisting of sand and Barren Land, demonstrated lower temperatures in comparison to urbanized regions. Nevertheless, it exhibited the most elevated (LST) and (UHI) development between 2003 and 2013. From 2003 to 2023, urban green spaces had surface temperatures that were 1.4–4.7°C lower than the temperatures in the transition zones. The mean (LST) of Barren Land exhibited a significantly higher value compared to that of water bodies and vegetation, indicating a persistent upward trend in LST throughout time. In 2003, the average temperature in metropolitan areas was 48°C, and it gradually rose to around 50°C by 2023. This trend aligns with the findings of other researchers who have examined the relationship between (LST) and land use (LU) in urban regions.

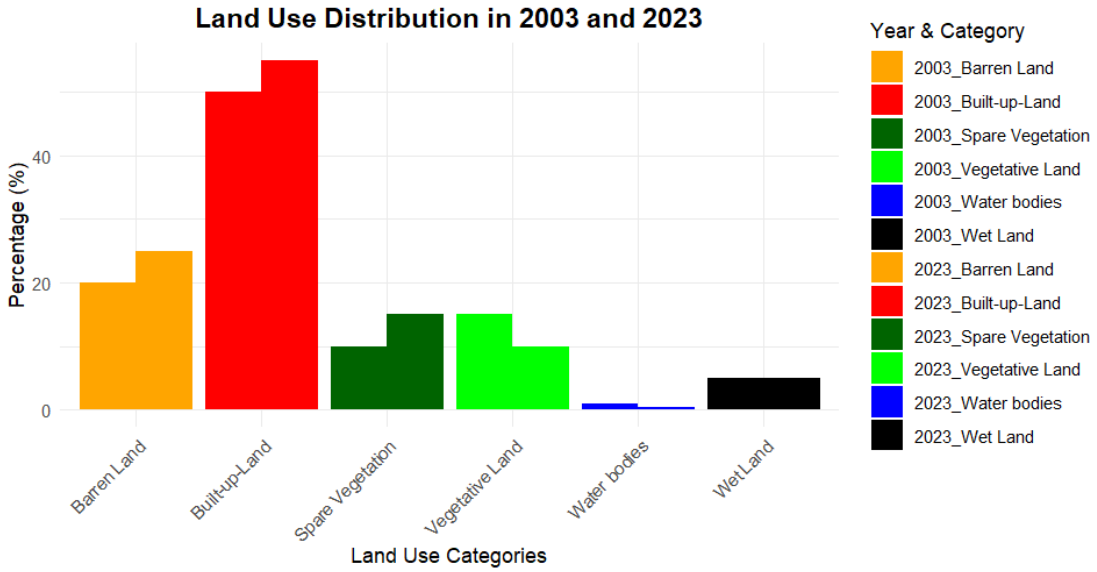

Figure 5 Temporal variation pattern of mean LST of LU classes in Malakand Division.

Comparison and Validation of (LST) Dynamics

Xiong and Chen (2017) employed surface temperature data acquired during image retrieval and air temperature data from the Pakistan Meteorological Department (PMD) meteorological station to compare and authenticate the (LST) derived from Landsat satellite images. Xiong and Chen (2017) utilized surface temperature data obtained on the same day as the image retrieval, along with air temperature data from the Pakistan Meteorological Department (PMD) meteorological station, to compare and veri fy the Land Surface Temperature (LST) produced from Landsat satellite images.

Table 5 displays a comparison of air temperature and land surface temperature. The inclusion of positive and negative integers signifies whether the temperature obtained from the weather station data is more or lesser than the image-derived LST, correspondingly. The observed variances ranged from 2 to 3 degrees Celsius, providing validation for the precision of the Land Surface Temperature (LST) obtained from satellite data (Fu & Weng, 2016; Qin QiMing et al., 2011; Xiong & Chen, 2017).

Land Use Metrics and Indices

The research region was analyzed using three indicators of land use: NDBI, NDVI, and NDWI. The purpose was to examine the link between LST, UHI, and land modification. This analysis is shown in Figure 7. The NDVI maps (Fig. 7) indicate a decline in urban vegetation cover throughout the study area between 2003 and 2023. The south and north portions are predominantly covered by agricultural land, with high NDVI values. The central, southern, and other locations have low NDVI values due to different land use and land cover classes. Figure 6 depicts the gradual reduction in the amount of vegetation in the Malakand Division caused by the spread of urban areas and alterations to the topography.

Redish places on the map show built-up areas and various land use and cover classes, whereas green areas indicate the presence of healthy vegetation cover and green spaces. The NDBI maps (Fig. 7) demonstrate a consistent expansion of urban built-up land across the whole research area between 2003 and 2023. Elevated NDBI levels are detected in the center area of the region. The NDWI maps (Fig. 7) illustrate a progressive drop in NDWI values attributed to urban growth. The NDWI values for the years 2003, 2013, and 2023 were 1.601, 1.411, and 1.10321, respectively. The UHI study utilizes these three indicators due to their ability to showcase the influence of urban expansion on the study area.

Table 5 Surface temperature and air comparison.

Date	LST (RMC) Peshawar PBO	Air temperature	Surface temperature and air difference
18–03-2003	15.68	14.75	0.93
07–03-2013	11.44	10.05	1.39
15–03-2023	09.71	08.2	1.51
Date	LST (Met observatory Timergara Lower Dir)	Air temperature	Surface temperature and air difference
18–03-2003	14.25	12.45	1.80
07–03-2013	11.31	08.5	2.81
15–03-2023	12.68	11.2	1.48

The studied region is greatly affected by temperature variations, which play a crucial role in the formation of UHI.

UHI Intensity Analysis

Khorrami and Gunduz (2020) categorized the power of UHI into five distinct levels: extraordinarily low, low, moderate, high, and exceedingly, as determined by their research. Figure 8 illustrates the regional and temporal variations in (UHI) intensity in Metropolitan areas from 2003 to 2023. The results showed an instance of urban heat island (UHI) effect in the very low category that initially increased and subsequently decreased during the past twenty years (2003: 09.02%; 2013: 10.10%; 2023: 12.33%).

The category with low (UHI) intensity showed varying patterns over the years (2003: 14.41%; 2013: 22.35%; 2023: 19.88%). The intensity of the (UHI) at a moderate level declined with time, with percentages of 10.98% in 2003, 15.04% in 2013, and 18.09% in 2023. In contrast, the intensity of the UHI at a high level almost quadrupled, with percentages of 22.80% in 2003, 30.30% in 2013, and 30.58% in 2023. Similarly, the UHI category at a very high level exhibited a consistent upward trend, with percentages of 15.96% in 2003, 22.21% in 2013, and 19.08% projected for 2023, as indicated in Table 6.

The study's land-use analysis revealed an increasing proportion of urban regions, resulting in a decline in other land uses. The growth of urban areas and the decrease in natural vegetation and barren land have led to a rise in both LST and UHI) intensity throughout time. This phenomenon indicates a shift in land utilization, where developed areas are growing while plant cover, barren ground, marshes, and water bodies are diminishing. As a result, surface temperatures in the urban microclimate are increasing. Figure 8 illustrates the visual representation of locations in Malakand Division that have been influenced by UHI) occurrence from 2003 to 2023.

Ecological Assessment of (UTFVI)

The Urban Thermal Field Variance Index (UTFVI) is a quantitative measure that examines the impact of Urban Heat Island on urban environments and quality of life. It specifically focuses on urban ecology and thermal comfort (Renard et al., 2019; Zhang et al., 2001) classified the UTFVI model into five distinct types. Figure 9 displays the Urban Thermal Field Variance Index map, which depicts the spatiotemporal patterns in thermal ecological evaluation. Regions with elevated levels of urban thermal field variability index (UTFVI) exhibit a noticeable increase in temperature compared to the surrounding areas. UTFVI is employed to evaluate the quality of urban ecology and the level of thermal comfort associated with urban heat island (UHI) effects.

Within the Malakand Division, specific regions experiencing significant heat stress (UTFVI > 0.203) and favorable microclimate conditions (UTFVI < 0) were found. In 2003, 09.02% of the region exhibited favorable circumstances, 14.41% displayed average conditions, and 10.98.80% experienced unfavorable conditions. The conditions that were considered worse accounted for 22.80%, while the conditions that were considered worst accounted for 15.96%. In 2023, the proportion of the good index area declined to 12%, the normal area decreased to 19.88%, the bad index decreased to 18.09%, while the worse condition area climbed to 30.58%, and the worst condition area increased to 19.08%.

According to Table 7, there was a substantial decrease of 3669.32 km² and 6104.94 km² in the areas classified as good and normal conditions, respectively, between 2003 and 2023. The index region of poor-quality spans 4942.04 km², while the areas with even worse and the most severe conditions have expanded by 8509.26 km² and 6067.86 km², respectively. These expansions are indicative of the intense heat conditions resulting from fast urbanization and development.

Investigating the Connection Between (LST) and Satellite Records

An examination was directed to look at the connection between various satellite land-use records (NDBI, NDVI, NDWI) and LST to get understanding into the metropolitan intensity island (UHI) impact and biological results in the concentrated-on region. Figure 10 shows the topographical dissemination of the connection between these pointers and LST. The relationship examination exhibited a strong association between Land Surface Temperature (LST) and Standardized Distinction Developed File (NDBI), Standardized Contrast Vegetation Record (NDVI), and Standardized Contrast Water File (NDWI). Figures 10 and 10 outline a negative association among NDVI and NDWI and LST, proposing that locales with more prominent vegetation and water content by and large display lower surface temperatures.

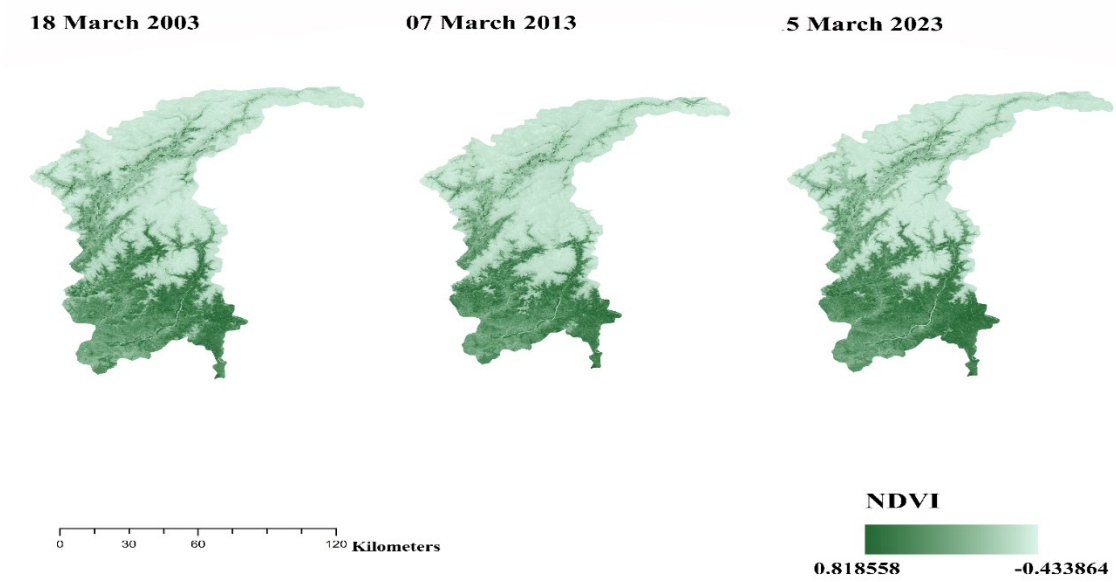
18 March 2003
07 March 2013
5 March 2023
0
30
60
120
Kilometers
NDVI
0.818558
-0.433864

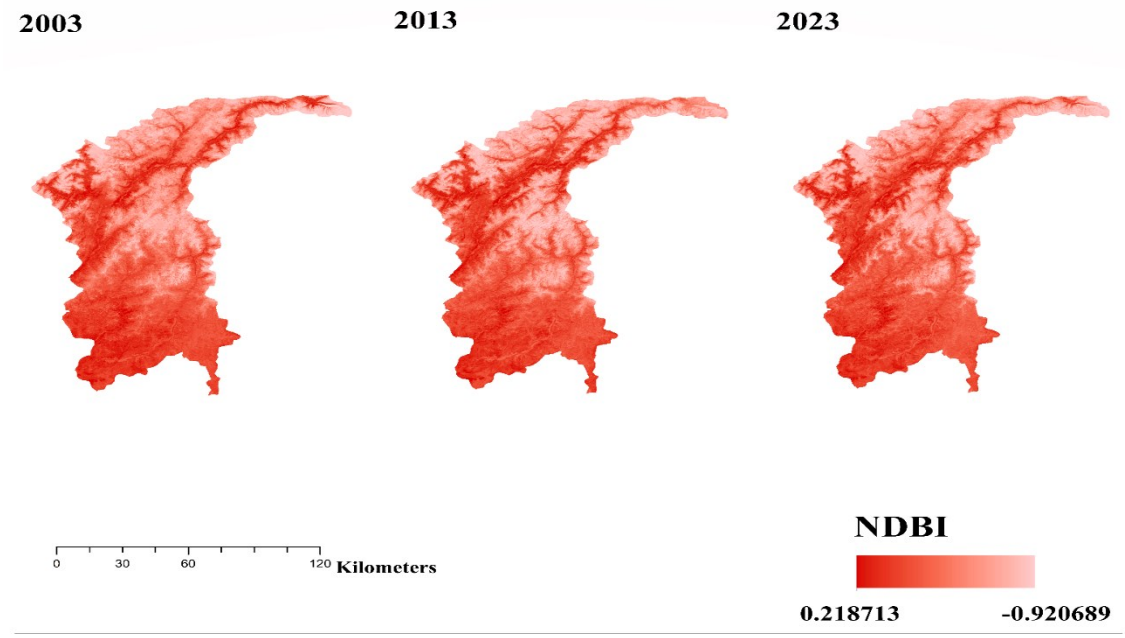
2003
2013
2023
0
30
60
120
Kilometers
NDBI
0.218713
-0.920689

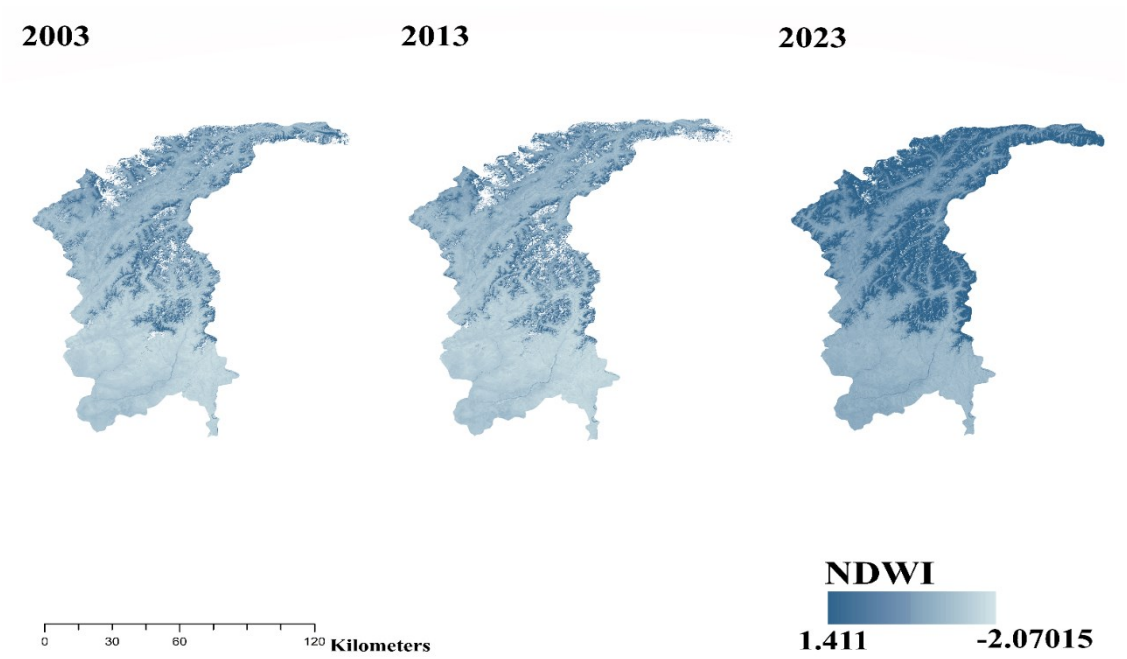

Figure 6 Land Use Indices of Malakand Division for the Years **2003**, **2013**, and **2023.**

The (LST) displays a powerful regrettable relationship with both vegetation and water bodies. As land surface temperature (LST) builds, there is a comparing drop in the extent of water bodies, exhibiting a negative relationship between these two variables. These findings indicate that the presence of vegetation and water bodies helps to sustain lower (LST) levels. The reduction in natural vegetation and water bodies is directly correlated with a rise in (LST), as depicted in Figure 10. Urbanization and human interference in Malakand Division have led to a reduction in flora and water resources, as evidenced by this chart.

Conversely, the NDBI pointer shows a good association with LST, as portrayed in Figure 10. As metropolitan regions grow, the (LST) increments. The significant development of metropolitan regions and the decrease in vegetation inclusion have brought about raised temperatures, showing a powerful connection between Territory Surface Temperature (LST) and Land Use (LU) records. More noteworthy backwoods inclusion and the presence of water bodies add to diminished Land Surface Temperature (LST), though the development of urbanized regions adds to raised LST. This connection shows the impact of the Metropolitan Intensity Island (UHI) impact in the examination area, where the extension of created regions and (LST) have consistently risen.

5. Discussions

This research investigates the meteorological and natural conditions of Malakand Division over the years 2003, 2013, and 2023. The research employs multi-temporal Landsat satellite imagery, following the methodology used in previous global research efforts (Amiri et al., 2009; Avdan & Jovanovska, 2016; Chen et al., 2006; Gazi & Mondal, 2018; Mokarram et al., 2023). In order to assess the ecological and climatic conditions of urban areas, particularly in important locations like Malakand Division, it is crucial to comprehend the many factors and their spatial and temporal patterns. The variables examined in this study include land use, variations in surface temperature,

impermeable layers, and the urban heat island effect (UTFVI) (Dilawar et al., 2021; Kafy, Rahman, et al., 2021; Malah & Bahi, 2022; Verma et al., 2020).

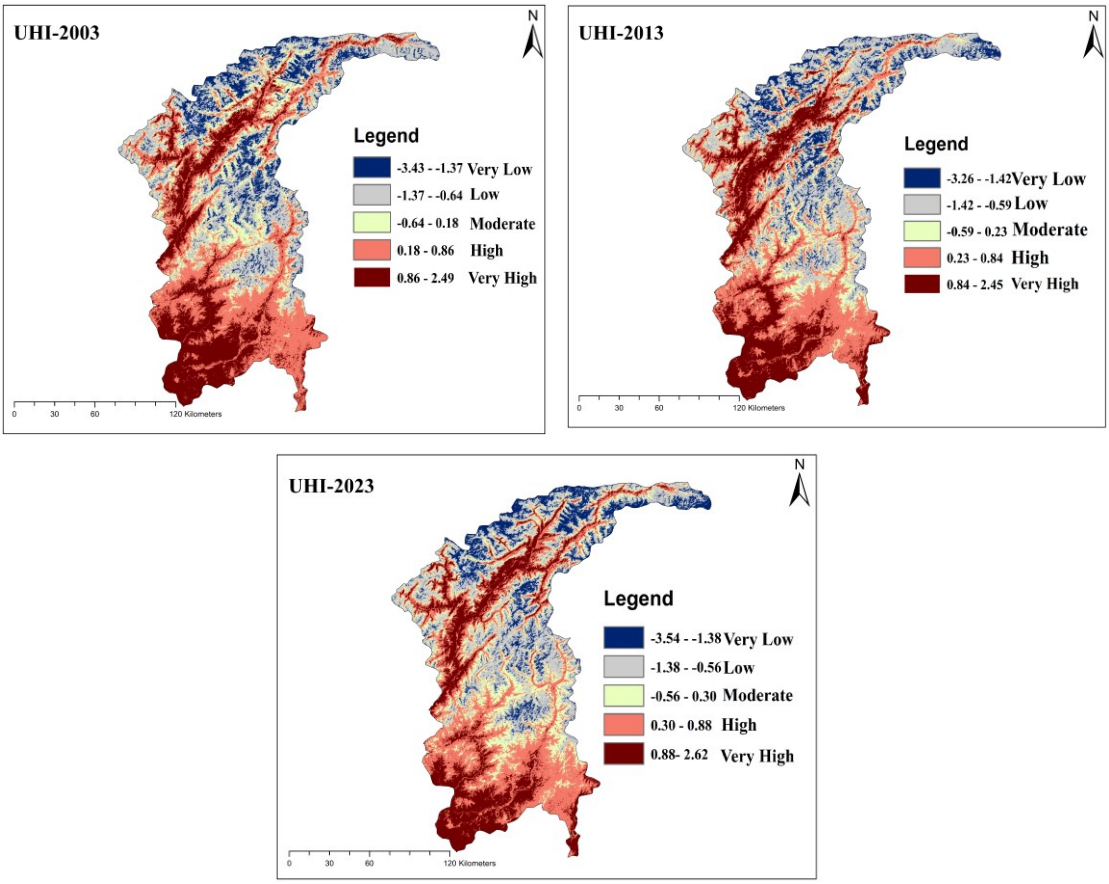

Figure 7 UHI of 2003, 2013 and 2023.

The findings of this study clearly demonstrate that changes in land use and land cover (LULC) in large urban areas are primarily driven by an increase in (UHI) effect, loss of biodiversity, and degradation of ecosystems. These perspectives fundamentally impact the overall well-being and daily living conditions of the residents. The indisputable outcomes are a reduction in vegetation coverage and an increase in both the lowest and highest temperatures, both of which directly impact the thermal conditions within urban areas.

Table 6 statistical Analysis of the (UHI) of Malakand Division (2003-2023).

UHI Intensity	2003 Area (km2)	%Age	2013 Area (km2)	%Age	2023 Area (km^2)	%Age
Very low	3369.32	9.02	2760.54	10.1	3369.05	12.33
Low	5378.69	14.41	6104.94	22.35	5432.01	19.88
Moderate	4098.19	10.98	4098.25	15.04	4942.04	18.09
High	8509.26	22.8	8282.19	30.3	8357.08	30.58
Very high	5958.35	15.96	6067.86	22.21	5212.03	19.08

The interaction between different land uses can occasionally affect a region's ability to adapt its development to its natural environment. The changes in land use, such as the expansion of urban areas and the reduction in agricultural land and vegetation, indicate growth. However, these

changes also emphasize the importance of implementing sustainable urban planning to prevent negative impacts on temperature and ecology.

Although the rise in urban areas is a favorable sign of urban expansion, it also has several adverse repercussions for the city's sustainability and environmental conditions. According to Table 3, there was a negative correlation between the growth in built-up area and the loss in vegetation, Barren land, and water bodies over the study period. These patterns have also been noted in other recent studies conducted in Malakand Division (Akhtar et al., 2020; Almas et al., 2005; Bhalli & Abdul Ghaffar, 2015; Bhatti et al., 2015; Mumtaz et al., 2020; Riaz et al., 2014). The shifts mentioned are also evident in the graphical representation of land utilization throughout time seen in Figure 4. The data indicate that the main factor contributing to the formation of (UHIs) in the examined region is urban expansion. The average (LST) of Malakand Division has increased by around 1.84°C per decade, a worrisome trend for both the residents and the local environment.

The rise in (LST) is directly linked to the depletion of open and green areas, farmland, and urban vegetation, as well as the expansion of impermeable surfaces and urban development. The combination of a high human density and packed structures has significantly increased surface temperatures. UHI hotspots are primarily concentrated in the northern and northeastern regions, as well as in building sites and densely populated ancient city neighborhoods. Comparable results have been documented in other urban areas of Pakistan, such as Karachi (Baqa et al., 2022), Faisalabad (Tariq & Shu, 2020), and Peshawar (Ahmad et al., 2022). While the increase in urban areas is a positive indicator of urban expansion, it also has several negative consequences for the city's sustainability and environmental conditions. According to Table 3, there was a negative correlation between the growth in developed regions and the loss of vegetation, Barren land, and water bodies during the study period. These cases have also been documented in other recent studies conducted in Malakand Division (Akhtar et al., 2020; Almas et al., 2005; Bhatti et al., 2015; Ghaffar, 2015; Mumtaz et al., 2020; Riaz et al., 2014). The mentioned motions are also clearly evident in the graphical representation of changes in land usage over time depicted in Figure 4. The data indicates that urban expansion is the primary factor contributing to the establishment of (UHIs) in the studied area. The average Land Surface Temperature (LST) of Malakand Division has increased by around 1.84°C every decade, which is a concerning trend for both the residents and the local climate.

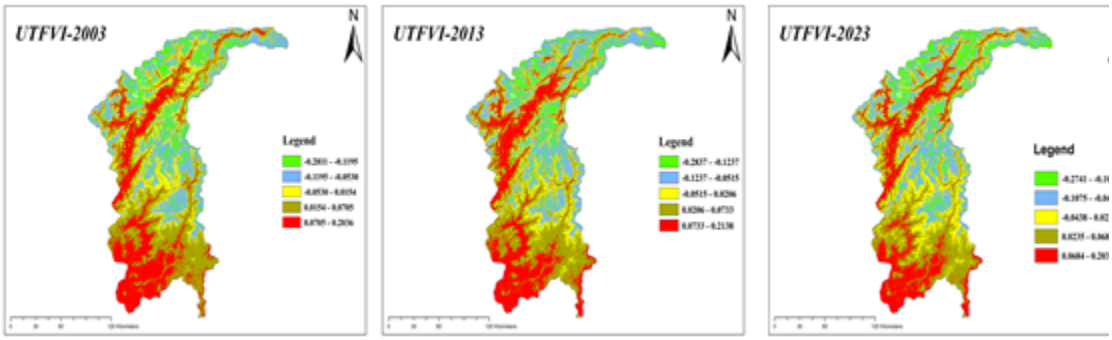

Figure 8 UTFVI of 2003, 2013 and 2023.

The increase in land surface temperature (LST) is directly linked to the loss of open and green areas, farms, and urban vegetation, as well as the expansion of impermeable surfaces and urban development. The combination of a high population density and densely built structures has significantly elevated surface temperatures. The areas of interest for UHI are primarily concentrated

in the northern and northeastern regions, as well as in urban areas with high building density and densely populated historic city centers.

The research reveals an increase in the (UHI) phenomenon due to rising land surface temperatures (LST) caused by changes in land use, specifically the large expansion of built-up areas and the reduction of green spaces. From 2005 to 2020, a doctoral researcher specializing in scene design conducted an intensive study in Tianjin, China. The study employed geospatial approaches and discovered that changes in land-use cover and human activities have a significant impact on the geographical distribution of Land Surface Temperature (LST).

Table 7 UTFVI and temporal variation in the region under UTFVI.

UTFVI EEI	2003 Area (km2)	%Age	2013 Area (km2)	%Age	2023 Area (km2)	%Age
-0.2741-0.1075 G	3369.32	9.02	2760.54	10.1	3369.05	12.33
-0.1075-0.0438 N	5378.69	14.41	6104.94	22.35	5432.01	19.88
-0.0438-0.0235 B	4098.19	10.98	4098.25	15.04	4942.04	18.09
0.0235-0.0684 W	8509.26	22.8	8282.19	30.3	8357.08	30.58
0.068-0.203 WO	5958.35	15.96	6067.86	22.21	5212.03	19.08

According to (Ullah et al., 2022), the review region is expected to see a temperature increase of 3.39°C throughout the review period. This study focuses on investigating the urban characteristics of the Kolkata district and its surrounding metropolitan and rural areas in India. These characteristics have been affected by both climate change and the rapid growth of urbanization. The study revealed that urban areas see a significant increase in temperature compared to rural areas, mostly attributed to factors such as high population density, industrialization, and decreased greenery (Halder et al., 2021).

Human activities are driving urbanization, resulting in significant alterations in land use and land cover (LULC). According to (Choudhury et al., 2023; Roy et al., 2022; Yeboah et al., 2017), these progressions are causing severe weather patterns in metropolitan areas such as the Shanghai metropolitan region in China, Accra in Ghana, and the Kamrup Metropolitan locality in Northeast India. Urbanization has led to major changes in (LST) by transforming rural land and developing metropolitan districts into unproductive or unused land. The review shows an increase in the highest recorded (LST) and a drop in the lowest recorded LST across the review period.

The correlation between different land-use characteristics and (LST) emphasizes the influence of (UHI) effect and environmental aspects in the study area. The research conducted by (Amiri et al., 2009; Guha et al., 2017) has identified remarkably similar associations. The concentration of impermeable surfaces in metropolitan areas contributes to the intensification of the (UHI) effect, whereas the presence of vegetation and water bodies helps to mitigate the (LST).

Overall, there were substantial alterations in land utilization within the examined region between 2003 and 2023. The urbanized region experienced an 8% growth, while the amount of vegetation and barren terrain decreased by 4% and 3% respectively. The transformation of horticulture land and natural vegetation into developed areas, coupled with the decrease in barren land and water

bodies, has altered the radiation properties of the Earth's surface and resulted in ecological damage (Lyu et al., 2018). Urban areas and surfaces that do not allow water to pass through them have a great capacity to retain heat, which they then release during the evening. In contrast, vegetation and surfaces that allow water to pass through them cool down fast due to their low heat storage and evapotranspiration. Urban growth is mostly responsible for the increase in warm pressure in the exploring zone. Enhancing vegetation can serve as a prolonged method to alleviate the impacts of (LST) and urban heat islands.

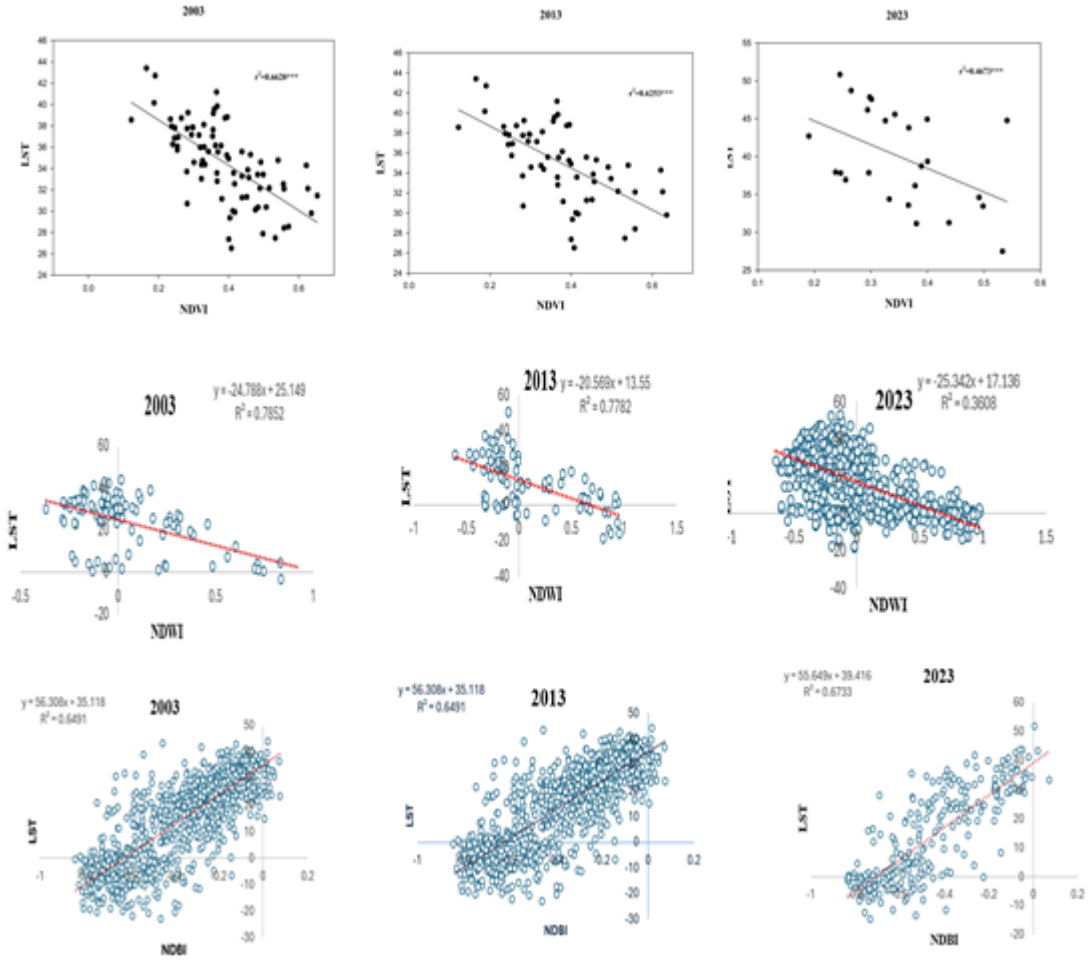

Figure 9 Correlation of Land use indecies.

Furthermore, the analysis acknowledges two distinct circumstances in Malakand Division: districts experiencing significant intensity stress and regions with optimal microclimates. Over time, there has been a decline in the number of locations with excellent and average warm conditions, while the number of locations with poor and very poor warm conditions has increased, notably in the year 2023. The findings are consistent with research conducted in several regions, including Tehran in Iran, Mekelle City in Northern Ethiopia, and Dhaka, the capital city of Bangladesh (Hishe et al., 2024; Najafzadeh et al., 2021; Tesfamariam et al., 2023; Uddin et al., 2022). Therefore, the examination emphasizes the importance of implementing practical land-use planning and urban greening strategies, such as urban forests and green roofs, to mitigate the (UHI) effect and enhance the ecological condition of the city (Sanchez & Reames, 2019; Zhang & He, 2021).

6.Conclusion

Overall, there were substantial alterations in land utilization within the examined region between 2003 and 2023. The urbanized region experienced an 11773.5 km^2 to 12519.09 km^2 increase in development, while the amount of greenery and desert terrain decreased by 4091.19 km^2 to 3786.24 km^2 and 27.71% to23.24% accordingly. The conversion of horticultural areas and natural flora into developed regions, accompanied by the reduction of barren areas and water bodies, has modified the radiation characteristics of the Earth's surface and led to ecological harm (Lyu et al., 2018). Impervious urban areas and impermeable surfaces possess a high heat retention capacity, which they subsequently emit during the nighttime hours. On the other hand, vegetation and permeable surfaces cool down quickly since they have a low capacity to store heat and promote evapotranspiration. The expansion of urban areas is primarily responsible for the rise in atmospheric pressure in the exploration zone. Improving vegetation can be a long-term approach to mitigate the effects of land surface temperature

Furthermore, the analysis identifies two specific situations in Malakand Division: areas experiencing significant intensity pressure and regions with favorable microclimates. Over time, there has been a decline in the number of locations that have favorable and average warm conditions, while the number of areas with unfavorable and extremely unfavorable warm conditions has increased, particularly in the year 2023. The findings are consistent with studies conducted in other regions, including Tehran in Iran, Mekelle City in Northern Ethiopia, and Dhaka, the capital city of Bangladesh (Hishe et al., 2024; Najafzadeh et al., 2021; Tesfamariam et al., 2023; Uddin et al., 2022). The assessment emphasizes the importance of implementing practical land-use planning and urban greening strategies, such as urban forests and green rooftops, to reduce the (UHI) effect and enhance the environmental condition of the city (Sanchez & Reames, 2019; Zhang & He, 2021).

The results indicate that (LST) has increased in numerous regions of Malakand Division, irrespective of their rural or urban characteristics. The significant increase in (LST) highlights the extensive influence of urbanization and land use changes on the high temperatures of the region. The region's inherent environmental integrity is completely compromised by unfeasible alterations in land use resulting from industrialization and urbanization. These changes result in a reduction in native vegetation and open areas, which intensifies the (UHI) phenomenon and impacts human thermal well-being.

Understanding the elements that influence (LST) in this study is essential for assisting policymakers in developing ways to mitigate the (UHI) phenomenon. Urban greening solutions are increasingly essential remedies for managing the escalating Area Surface Temperature (LST) and its associated effects. It is advisable to introduce urban forests, roadside trees, green roofs, vertical forests, and tree canopy systems to enhance the amount of vegetation in Malakand Division and other regions of Pakistan. Implementing these technologies can mitigate the (UHI) effect by increasing the amount of vegetation, hence reducing the Surface Area Temperature (SAT) and enhancing human thermal comfort. In addition, it is widely recognized as a crucial approach to replace human-made structures with materials that have a low thermal conductivity and a high albedo. These materials can reduce the ability to retain and sustain intensity, resulting in a drop in the overall Land Surface Temperature (LST) in urban areas. By integrating these materials into a metropolitan design and development, networks can mitigate the (UHI) effect and create more sustainable and aesthetically pleasing urban settings.

This examination provides significant insights for politicians, ecologists, geographers, and urban planners. The results emphasize the urgent need for sustainable urban development strategies that

prioritize the protection of ecosystems and the provision of thermal comfort. Stakeholders may make well-informed decisions and strategize for the future development of Malakand Division and similar places by understanding the relationship between land use, (LST), and the (UHI) effect. The review explores the incorporation of environmentally-friendly framework and sustainable building materials into urban planning to promote long-lasting sustainable development. The findings of this study are essential for providing crucial information to city officials and urban planners in designing a sustainable urban land development strategy. Investing in public green spaces in urban areas reduces the (UHI) effect and enhances the ecological and thermal conditions of the area. The findings of the poll emphasize the importance of adopting a comprehensive approach to urban development that considers both the economic advantages of urbanization and the environmental and climatic consequences.

This study provides a comprehensive analysis of the meteorological and biological conditions in the Malakand Division for a period exceeding twenty years. The rapid urbanization of regions has led to a significant increase in (LST) and the intensification of the (UHI) phenomenon, while water bodies, deserted land, and vegetation cover have simultaneously decreased. The findings emphasize the crucial role of plants and bodies of water in mitigating the (UHI) effect and underscore the need for equitable urban growth practices. To mitigate the impact of (UHI) and promote economic development, policymakers and urban planners should implement urban greening measures and utilize materials with low thermal conductivity and high albedo. This study provides crucial guidance to stakeholders in making informed decisions to improve the environmental and climatic conditions of Malakand Division and other regions facing similar challenges.

Acknowledgment

This research was supported by a grant from the Education Department of Jilin Province, China, grant number JJKH20211289KJ, and the Natural Science Foundation of Jilin Scientific Institute of China grant number 20220101155JC.

References

Ahmad, A., & Quegan, S. (2012). Analysis of maximum likelihood classification on multispectral data. *Applied Mathematical Sciences*, *6*(129), 6425-6436.

Ahmad, N., Waqas, T., Shafique, M., & Ullah, I. (2022). The land surface temperature dynamics and Its impact on land cover in district Peshawar, Khyber Pakhtunkhwa. *International Journal of Environment and Geoinformatics*, *9*(3), 97-107.

Akhtar, M., Zhao, Y., Gao, G., Gulzar, Q., Hussain, A., & Samie, A. (2020). Assessment of ecosystem services value in response to prevailing and future land use/cover changes in Lahore, Pakistan. *Regional Sustainability*, *1*(1), 37-47.

Alfraihat, R., Mulugeta, G., & Gala, T. (2016). Ecological evaluation of urban heat island in Chicago City, USA. *Journal of Atmospheric Pollution*, *4*(1), 23-29.

Almas, A. S., Rahim, C., Butt, M., & Shah, T. I. (2005). Metropolitan growth monitoring and land use classification using geospatial techniques. Proceedings of international workshop on service and application of spatial data infrastructure, Hangzhou, China,

Amiri, R., Weng, Q., Alimohammadi, A., & Alavipanah, S. K. (2009). Spatial–temporal dynamics of land surface temperature in relation to fractional vegetation cover and land use/cover in the Tabriz urban area, Iran. *Remote sensing of environment*, *113*(12), 2606-2617.

Avdan, U., & Jovanovska, G. (2016). Algorithm for automated mapping of land surface temperature using LANDSAT 8 satellite data. *Journal of sensors*, *2016*(1), 1480307.

Baqa, M. F., Lu, L., Chen, F., Nawaz-ul-Huda, S., Pan, L., Tariq, A., Qureshi, S., Li, B., & Li, Q. (2022). Characterizing spatiotemporal variations in the urban thermal environment related to land cover changes in Karachi, Pakistan, from 2000 to 2020. *Remote Sensing*, *14*(9), 2164.

Bhalli, M., & Abdul Ghaffar, A. G. (2015). Use of geospatial techniques in monitoring urban expansion and land use change analysis: a case of Lahore, Pakistan.

Bhatti, S. S., Tripathi, N. K., Nitivattananon, V., Rana, I. A., & Mozumder, C. (2015). A multi-scale modeling approach for simulating urbanization in a metropolitan region. *Habitat International*, *50*, 354-365.

Buchori, I. The spatio-temporal trends of urban growth and surface urban heat islands over two decades in the Semarang Metropolitan Region.

Chen, X.-L., Zhao, H.-M., Li, P.-X., & Yin, Z.-Y. (2006). Remote sensing image-based analysis of the relationship between urban heat island and land use/cover changes. *Remote sensing of environment*, *104*(2), 133-146.

Choudhury, U., Singh, S. K., Kumar, A., Meraj, G., Kumar, P., & Kanga, S. (2023). Assessing land use/land cover changes and urban heat island intensification: A case study of Kamrup Metropolitan District, Northeast India (2000–2032). *Earth*, *4*(3), 503-521.

Corner, R. J., Dewan, A. M., & Chakma, S. (2014). Monitoring and prediction of land-use and land-cover (LULC) change. *Dhaka megacity: geospatial perspectives on urbanisation, environment and health*, 75-97.

Dilawar, A., Chen, B., Trisurat, Y., Tuankrua, V., Arshad, A., Hussain, Y., Measho, S., Guo, L., Kayiranga, A., & Zhang, H. (2021). Spatiotemporal shifts in thermal climate in responses to urban cover changes: A-case analysis of major cities in Punjab, Pakistan. *Geomatics, Natural Hazards and Risk*, *12*(1), 763-793.

Fu, P., & Weng, Q. (2016). A time series analysis of urbanization induced land use and land cover change and its impact on land surface temperature with Landsat imagery. *Remote sensing of environment*, *175*, 205-214.

Ghaffar, A. (2015). Use of geospatial techniques in monitoring urban expansion and land use change analysis: A case of Lahore, Pakistan. *Journal of Basic & Applied Sciences*, *11*, 265-273.

Gherraz, H., Guechi, I., & Alkama, D. (2020). Quantifying the effects of spatial patterns of green spaces on urban climate and urban heat island in a semi-arid climate. *Bulletin de la Société Royale des Sciences de Liège*.

Guha, S., Govil, H., Dey, A., & Gill, N. (2018). Analytical study of land surface temperature with NDVI and NDBI using Landsat 8 OLI and TIRS data in Florence and Naples city, Italy. *European Journal of Remote Sensing*, *51*(1), 667-678.

Guha, S., Govil, H., & Mukherjee, S. (2017). Dynamic analysis and ecological evaluation of urban heat islands in Raipur city, India. *Journal of Applied Remote Sensing*, *11*(3), 036020-036020.

Halder, B., Bandyopadhyay, J., & Banik, P. (2021). Monitoring the effect of urban development on urban heat island based on remote sensing and geo-spatial approach in Kolkata and adjacent areas, India. *Sustainable Cities and Society*, *74*, 103186.

Hishe, S., Gidey, E., Zenebe, A., Girma, A., Dikinya, O., Sebego, R., & Lyimo, J. (2024). Urban heat island and ecological condition modeling using thermal remote sensing in Tigray–Northern Ethiopia. *Modeling Earth Systems and Environment*, *10*(1), 735-749.

Imran, H., Hossain, A., Shammas, M. I., Das, M. K., Islam, M. R., Rahman, K., & Almazroui, M. (2022). Land surface temperature and human thermal comfort responses to land use dynamics in Chittagong city of Bangladesh. *Geomatics, Natural Hazards and Risk*, *13*(1), 2283-2312.

Jain, M., Dimri, A., & Niyogi, D. (2017). Land-air interactions over urban-rural transects using satellite observations: analysis over Delhi, India from 1991–2016. *Remote Sensing*, *9*(12), 1283.

Joshi, J. P., & Bhatt, B. (2012). Estimating temporal land surface temperature using remote sensing: A study of Vadodara urban area, Gujarat. *International Journal of Geology, Earth and Environmental Sciences*, *2*(1), 123-130.

Kafy, A.-A., Al Rakib, A., Akter, K. S., Jahir, D. M. A., Sikdar, M. S., Ashrafi, T. J., Mallik, S., & Rahman, M. M. (2021). Assessing and predicting land use/land cover, land surface temperature and urban thermal field variance index using Landsat imagery for Dhaka Metropolitan area. *Environmental Challenges*, *4*, 100192.

Kafy, A.-A., Rahman, M. S., Islam, M., Al Rakib, A., Islam, M. A., Khan, M. H. H., Sikdar, M. S., Sarker, M. H. S., Mawa, J., & Sattar, G. S. (2021). Prediction of seasonal urban thermal field variance index using machine learning algorithms in Cumilla, Bangladesh. *Sustainable Cities and Society*, *64*, 102542.

Liu, Y., Li, Q., Yang, L., Mu, K., Zhang, M., & Liu, J. (2020). Urban heat island effects of various urban morphologies under regional climate conditions. *Science of the Total Environment*, *743*, 140589.

López, E., Bocco, G., Mendoza, M., & Duhau, E. (2001). Predicting land-cover and land-use change in the urban fringe: A case in Morelia city, Mexico. *Landscape and urban planning*, *55*(4), 271-285.

Lyu, R., Zhang, J., Xu, M., & Li, J. (2018). Impacts of urbanization on ecosystem services and their temporal relations: a case study in Northern Ningxia, China. *Land use policy*, *77*, 163-173.

Maithani, S., Nautiyal, G., & Sharma, A. (2020). Investigating the effect of lockdown during COVID-19 on land surface temperature: study of Dehradun city, India. *Journal of the Indian Society of Remote Sensing*, *48*, 1297-1311.

Malah, A., & Bahi, H. (2022). Integrated multivariate data analysis for Urban Sustainability Assessment, a case study of Casablanca city. *Sustainable Cities and Society*, *86*, 104100.

Martin, P., Baudouin, Y., & Gachon, P. (2015). An alternative method to characterize the surface urban heat island. *International journal of biometeorology*, *59*, 849-861.

Meshesha, T. W., Tripathi, S., & Khare, D. (2016). Analyses of land use and land cover change dynamics using GIS and remote sensing during 1984 and 2015 in the Beressa Watershed Northern Central Highland of Ethiopia. *Modeling Earth Systems and Environment*, *2*, 1-12.

Mohajerani, A., Bakaric, J., & Jeffrey-Bailey, T. (2017). The urban heat island effect, its causes, and mitigation, with reference to the thermal properties of asphalt concrete. *Journal of environmental management*, *197*, 522-538.

Mokarram, M., Taripanah, F., & Pham, T. M. (2023). Investigating the effect of surface urban heat island on the trend of temperature changes. *Advances in Space Research*, *72*(8), 3150-3169.

Mumtaz, F., Tao, Y., de Leeuw, G., Zhao, L., Fan, C., Elnashar, A., Bashir, B., Wang, G., Li, L., & Naeem, S. (2020). Modeling spatio-temporal land transformation and its associated impacts on land surface temperature (LST). *Remote Sensing*, *12*(18), 2987.

Naim, M. N. H., & Kafy, A.-A. (2021). Assessment of urban thermal field variance index and defining the relationship between land cover and surface temperature in Chattogram city: A remote sensing and statistical approach. *Environmental Challenges*, *4*, 100107.

Najafzadeh, F., Mohammadzadeh, A., Ghorbanian, A., & Jamali, S. (2021). Spatial and temporal analysis of surface urban heat island and thermal comfort using landsat satellite images between 1989 and 2019: A case study in Tehran. *Remote Sensing*, *13*(21), 4469.

Nath, B., Wang, Z., Ge, Y., Islam, K., P. Singh, R., & Niu, Z. (2020). Land use and land cover change modeling and future potential landscape risk assessment using Markov-CA model and analytical hierarchy process. *ISPRS International Journal of Geo-Information*, *9*(2), 134.

Nguyen, T. M., Lin, T.-H., & Chan, H.-P. (2019). The environmental effects of urban development in Hanoi, Vietnam from satellite and meteorological observations from 1999–2016. *Sustainability*, *11*(6), 1768.

Oke, T. R. (1976). The distinction between canopy and boundary-layer urban heat islands. *Atmosphere*, *14*(4), 268-277.

Portela, C. I., Massi, K. G., Rodrigues, T., & Alcântara, E. (2020). Impact of urban and industrial features on land surface temperature: Evidences from satellite thermal indices. *Sustainable Cities and Society*, *56*, 102100.

Qin, Q., Zhang, N., Nan, P., & Chai, L. (2011). Geothermal area detection using Landsat ETM+ thermal infrared data and its mechanistic analysis—A case study in Tengchong, China. *International Journal of Applied Earth Observation and Geoinformation*, *13*(4), 552-559.

Qin QiMing, Q. Q., Zhang Ning, Z. N., Nan Peng, N. P., & Chai LeiLei, C. L. (2011). Geothermal area detection using Landsat ETM+ thermal infrared data and its mechanistic analysis-a case study in Tengchong, China.

Qu, S., Wang, L., Lin, A., Yu, D., & Yuan, M. (2020). Distinguishing the impacts of climate change and anthropogenic factors on vegetation dynamics in the Yangtze River Basin, China. *Ecological Indicators*, *108*, 105724.

Qureshi, J., Mahmood, S. A., Almas, A. S., Rafique, H. M., & Irshad, R. (2012). Monitoring spatiotemporal and micro-level climatic variations in Lahore and subrubs using satellite imagery and multi-source data. *Journal of Faculty of Engineering & Technology*, *19*(1), 51-65.

Renard, F., Alonso, L., Fitts, Y., Hadjiosif, A., & Comby, J. (2019). Evaluation of the effect of urban redevelopment on surface urban heat islands. *Remote Sensing*, *11*(3), 299.

Riaz, O., Ghaffar, A., & Butt, I. (2014). Modelling land use patterns of Lahore (Pakistan) using remote sensing and GIS. *Global Journal of Science Frontier Research. Environment & Earth Science*, *14*(1), 24-30.

Rooney, C., McMichael, A. J., Kovats, R. S., & Coleman, M. P. (1998). Excess mortality in England and Wales, and in Greater London, during the 1995 heatwave. *Journal of Epidemiology & Community Health*, *52*(8), 482-486.

Roy, P. S., Ramachandran, R. M., Paul, O., Thakur, P. K., Ravan, S., Behera, M. D., Sarangi, C., & Kanawade, V. P. (2022). Anthropogenic land use and land cover changes—A review on its environmental consequences and climate change. *Journal of the Indian Society of Remote Sensing*, *50*(8), 1615-1640.

Sahana, M., Ahmed, R., & Sajjad, H. (2016). Analyzing land surface temperature distribution in response to land use/land cover change using split window algorithm and spectral radiance model in Sundarban Biosphere Reserve, India. *Modeling Earth Systems and Environment*, *2*, 1-11.

Sameen, M. I., & Al Kubaisy, M. A. (2014). Automatic surface temperature mapping in arcgis using landsat-8 tirs and envi tools, case study: Al Habbaniyah Lake. *J. Environ. Earth Sci*, *4*(12), 12-17.

Sanchez, L., & Reames, T. G. (2019). Cooling Detroit: A socio-spatial analysis of equity in green roofs as an urban heat island mitigation strategy. *Urban Forestry & Urban Greening*, *44*, 126331.

Sekertekin, A., Kutoglu, S. H., & Kaya, S. (2016). Evaluation of spatio-temporal variability in Land Surface Temperature: A case study of Zonguldak, Turkey. *Environmental monitoring and assessment*, *188*, 1-15.

Shah, B., & Ghauri, B. (2015). Mapping urban heat island effect in comparison with the land use, land cover of Lahore district. *Pakistan Journal of Meteorology Vol*, *11*(22), 37-48.

Shakrullah, K. (2021). Impact of land-use changes on the temperature variability: A case study of Lahore. *Pakistan Journal of Science*, *73*(2).

Sharma, R., Pradhan, L., Kumari, M., & Bhattacharya, P. (2021). Assessing urban heat islands and thermal comfort in Noida City using geospatial technology. *Urban Climate*, *35*, 100751.

Singh, P., Kikon, N., & Verma, P. (2017). Impact of land use change and urbanization on urban heat island in Lucknow city, Central India. A remote sensing based estimate. *Sustainable Cities and Society*, *32*, 100-114.

Sobrino, J. A., & Irakulis, I. (2020). A methodology for comparing the surface urban heat island in selected urban agglomerations around the world from Sentinel-3 SLSTR data. *Remote Sensing*, *12*(12), 2052.

Sobrino, J. A., Jiménez-Muñoz, J. C., & Paolini, L. (2004). Land surface temperature retrieval from LANDSAT TM 5. *Remote sensing of environment*, *90*(4), 434-440.

Talukdar, S., Singha, P., Mahato, S., Pal, S., Liou, Y.-A., & Rahman, A. (2020). Land-use land-cover classification by machine learning classifiers for satellite observations—A review. *Remote Sensing*, *12*(7), 1135.

Tariq, A., & Shu, H. (2020). CA-Markov chain analysis of seasonal land surface temperature and land use land cover change using optical multi-temporal satellite data of Faisalabad, Pakistan. *Remote Sensing*, *12*(20), 3402.

Tesfamariam, S., Govindu, V., & Uncha, A. (2023). Spatio-temporal analysis of urban heat island (UHI) and its effect on urban ecology: The case of Mekelle city, Northern Ethiopia. *Heliyon*, *9*(2).

Thi Mai Nguyen, T. M. N., Lin TangHuang, L. T., & Chan HaiPo, C. H. (2019). The environmental effects of urban development in Hanoi, Vietnam from satellite and meteorological observations from 1999-2016.

Uddin, A. S., Khan, N., Islam, A. R. M. T., Kamruzzaman, M., & Shahid, S. (2022). Changes in urbanization and urban heat island effect in Dhaka city. *Theoretical and Applied Climatology*, *147*(3), 891-907.

Ullah, N., Siddique, M. A., Ding, M., Grigoryan, S., Zhang, T., & Hu, Y. (2022). Spatiotemporal impact of urbanization on urban heat island and urban thermal field variance index of Tianjin City, China. *Buildings*, *12*(4), 399.

Ullah, S., Tahir, A. A., Akbar, T. A., Hassan, Q. K., Dewan, A., Khan, A. J., & Khan, M. (2019). Remote sensing-based quantification of the relationships between land use land cover changes and surface temperature over the Lower Himalayan Region. *Sustainability*, *11*(19), 5492.

Venter, Z. S., Brousse, O., Esau, I., & Meier, F. (2020). Hyperlocal mapping of urban air temperature using remote sensing and crowdsourced weather data. *Remote sensing of environment*, *242*, 111791.

Verma, P., Singh, P., Singh, R., & Raghubanshi, A. (2020). *Urban ecology: emerging patterns and social-ecological systems*. Elsevier.

Voogt, J. A., & Oke, T. R. (2003). Thermal remote sensing of urban climates. *Remote sensing of environment*, *86*(3), 370-384.

Wemegah, C. S., Yamba, E. I., Aryee, J. N., Sam, F., & Amekudzi, L. K. (2020). Assessment of urban heat island warming in the greater accra region. *Scientific African*, *8*, e00426.

Xiong, Y., & Chen, F. (2017). Correlation analysis between temperatures from Landsat thermal infrared retrievals and synchronous weather observations in Shenzhen, China. *Remote Sensing Applications: Society and Environment*, *7*, 40-48.

Yeboah, F., Awotwi, A., Forkuo, E. K., & Kumi, M. (2017). Assessing the land use and land cover changes due to urban growth in Accra, Ghana. *Journal of Basic and Applied Research International*, *22*(2), 43-50.

Zhang, G., & He, B.-J. (2021). Towards green roof implementation: Drivers, motivations, barriers and recommendations. *Urban Forestry & Urban Greening*, *58*, 126992.

Zhang, X., Zhong, T., Feng, X., & Wang, K. (2009). Estimation of the relationship between vegetation patches and urban land surface temperature with remote sensing. *International Journal of Remote Sensing*, *30*(8), 2105-2118.

Zhang, Y., Yu, T., & Gu, X. (2001). Land surface temperature retrieval from cbers-02 irmss thermal infrared data and its applications in quantitative analysis of urban heat island effect.

Zia, S. (2014). Temporal analysis of temperature trends in the metropolitan area of Lahore, Pakistan. *Pakistan Journal of Science*, *66*(1).